Fatigue Damage Identification on Concrete Structures Using Modal Analysis

TOMAS PLACHY, MICHAL POLAK
Department of Mechanics, Faculty of Civil Engineering
Czech Technical University in Prague
Thakurova 7, Prague 6
CZECH REPUBLIC

Abstract: - The paper deals with three types of concrete elements and their fatigue damage identification. Three reinforced concrete beams, four reinforced concrete slabs and two prestressed concrete slabs were investigated. They were loaded by static and dynamic fatigue loading during which the location of the damage was monitored and written down. The loading was applied in steps and after each step, the complete modal analysis was done. Modal characteristics were evaluated after each step of loading. Damage identification was done by three different methods based on the evaluated modal characteristics. Results of these methods were compared with written down real damage and suitability of each method was evaluated.

Key-Words: Damage identification, Modal analysis, Fatigue, Cracks, Reinforced concrete, Prestressed concrete

1 Introduction

In present days, traffic speed increases, the number of vehicles rapidly increases and they are much heavier and structures become inherently weak. This is why dynamic forces and fatigue loads caused problems on structures. New methods for monitoring of structure conditions and damage detection of a structure at the earliest possible stage are needed. The advantage of methods, which use results of an experimental modal analysis for estimation of a degradation degree of a structure, is that they can be applied to complex structures. These methods are suitable to verify on simple structural elements where we know their damage state.

2 Description of tested elements

Tests of structural elements of three types were carried out in laboratories of Faculty of Civil Engineering CTU in Prague. The influence of damage increase of reinforced concrete beams, reinforced concrete slabs and prestressed concrete slabs on change of their modal characteristics was monitored.

2.1 Reinforced concrete beams

Three identical reinforced concrete beams with dimensions 4.5 m x 0.3 m x 0.2 m were prepared for the purpose of the test (Fig. 1). The beams were put on cast steel bearing to achieve a good agreement with theoretical boundary conditions. They were simply supported with the length of a span 4.0 m with cantilevered ends 0.25 m on both sides.

2.2 Reinforced concrete slabs

After the evaluation of the first test results of the beams the second tests of the slabs were designed. Four identical reinforced concrete slabs with dimensions 3.2 m x 1.0 m x 0.1 m were made for the purpose of the test (Fig. 2). Slabs were simply supported on two opposite sides with the span 3.0 m and cantilevered ends 0.1 m.

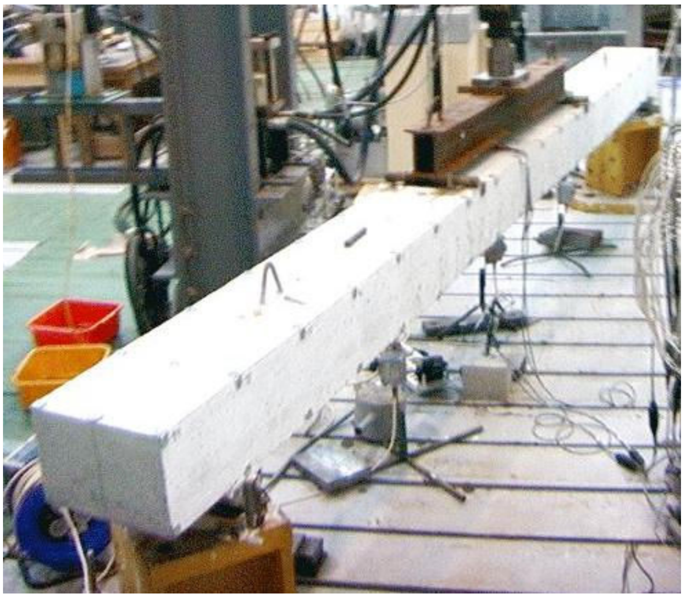

Fig.1 The reinforced concrete beam

2.3 Prestressed concrete slabs

The last test was done on two prestressed concrete slabs made by SMP CONSTRUCTION a.s. The dimensions of the slabs were 130 x 1155 x 4500 mm with ends expanded to the height 400 mm for embedment of the prestressing cables (Fig. 3). Slabs were made from concrete C45/55 with eleven prestressing cables of diameter 15.7 mm. The slabs were put on two bearing to be a simply supported with the span 3500 mm with cantilevered ends 500 mm on both sides (Fig. 3).

The tested slabs were designed as a fully prestressed concrete slabs according CSN EN 1992-1-1 to not comply with the safety condition for the fatigue loading in the lower part of the slab.

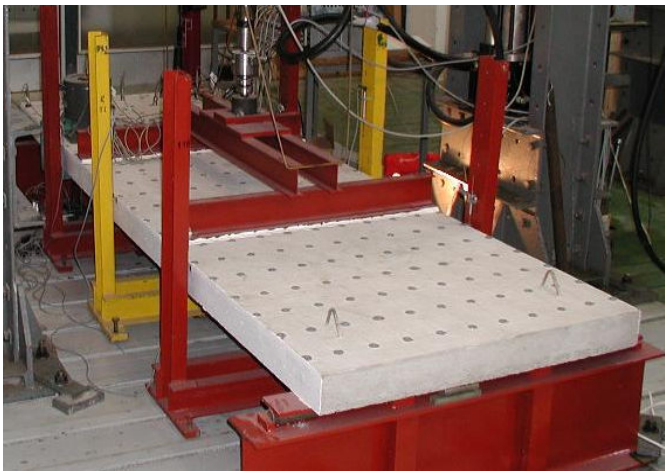

Fig.2 The reinforced concrete slabs

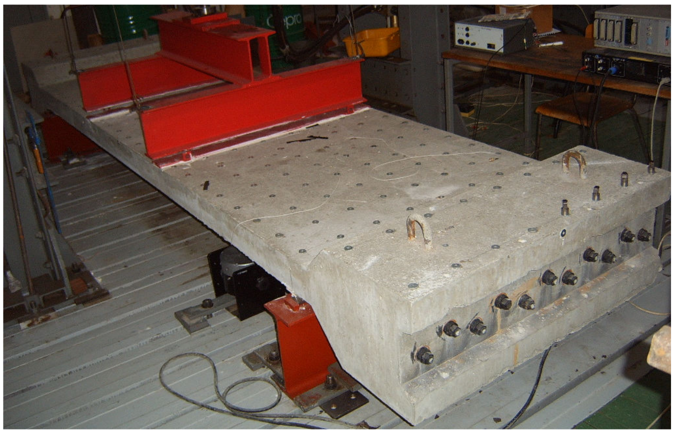

Fig.3 The prestressed concrete slabs

3 Loading of the tested elements

3.1 Reinforced concrete beams

The state deterioration of beams was done by static load and dynamic fatigue load. The beams were tested in four-point bending to get a constant bending moment in the mid-section of the beam (Fig. 1). Static load was imposed in four steps (load by its self-weight, load effect equals to a theoretical limit of the crack initiation, load to the first real cracking in the lower part of the beam, load to the half of the ultimate moment). Then we continued with a dynamic fatigue load, which was induced by harmonic force. The amplitude of the dynamic load was chosen to achieve a stress range in the main reinforcement $\Delta\sigma$ = 220 MPa, which would caused the end of a service life of the beam after 500 000 cycles. In the reality the end of the service life of the beam No. 1 came after 260 000 cycles (52% of the theoretical lifetime). So for the beams No. 2 and 3 the loading steps were divided into steps about 65 000 cycles. The end of the service life of the beam No. 2 came after 220 000 cycles (44% of the theoretical lifetime) and for the beam No. 3 came after 255 000 cycles (51% of the theoretical lifetime).

3.2 Reinforced concrete slabs

Slabs were also loaded by static and dynamic fatigue load. Static load was imposed in the same four steps as for beams but the steps for dynamic load were different. In contrary to the beams, the end of the fatigue life of the first slab came after 1 000 000 cycles (200% of the theoretical lifetime). Therefore, the fatigue load was done in four steps (load to the half of the theoretical lifetime – 250 000 cycles, load to the theoretical lifetime - 500 000 cycles, load to the 750 000 cycles and load to the end of the real lifetime). The end of the fatigue life of three remaining slabs was the same as for the first one.

3.3 Prestressed concrete slabs

Contrary to the previous reinforced concrete elements the prestressed concrete slabs were loaded only by dynamic fatigue load. The cyclic load was applied to the slabs in several steps. This fatigue load of the slabs was induced by harmonic force. The amplitude of the dynamic load was chosen to not comply with the safety condition for the fatigue loading of the concrete according to CSN EN 1992-1-1.

$$\frac{\sigma_{c,\max}}{f_{cd,fat}} \leq 0.5 + 0.45\frac{\sigma_{c,\min}}{f_{cd,fat}} \leq 0.9 \ , \qquad (1)$$

where $\sigma_{c,max}$ is the maximal compressive stress, $\sigma_{c,max}$ is the minimal compressive stress and $f_{cd,fat}$ is the design compressive strength of the concrete.

4 Data acquisition

4.1 Reinforced concrete beams

Before the test and after each load step the dynamic response of the beam was measured with a separate test arrangement. For the excitation of the beam during the experimental modal analysis the electrodynamic shaker ESE 11 076 was used. The shaker produced a random driving force over the frequency range of 5 to 200 Hz. The excitation force was measured indirectly by measuring the acceleration of the excitation mass. The acceleration transducer B12/200 HBM was placed on the excitation weight. The response of the elements onto forcing by the exciter was measured by ten inductive acceleration transducers B12/200 HBM in a chosen net of points (5 points in each of 19 cross sections) on the upper face in vertical direction and on the left side of the beam in horizontal direction.

The shaker was placed centrally to the longitudinal axis of the beam. It lies in the two fifths of the beam span. The position of the point of excitation was designed to be able to excite basic bending modes of natural vibration of the beam. Values of the Frequency Response Function $H_{rS}(if)$ were obtained as an average from ten measurements. The window length of the time signal processing was 16 s, the frequency range of the window was set to 200 Hz.

4.2 Reinforced concrete slabs

Before the test and after each load step the dynamic response of the slab was measured with a separate test arrangement as for the beams. The response of the slabs was measured only in vertical direction in a chosen net of points (11 points in each of 21 cross sections) on the upper face.

4.3 Prestressed concrete slabs

For the data acquisition of the reinforced concrete slabs the newer equipment Bruel & Kjaer was used.

The dynamic cyclic loading stopped after each 250 000 cycles and an experimental modal analysis was carried out. The Modal Exciter Type 2732 (Bruel & Kjaer) was used for the excitation of the prestressed concrete slab. The exciter was placed under the slab (Fig. 3) linked to the slab with the flexible drive rod. The exciter produced a random driving force over the frequency range of 5 to 400 Hz. The force transducer Endevco 2311-10 placed between the flexible rod and the slab measured the excitation force. The response of the element onto forcing by the exciter was measured by three piezoelectric acceleration transducers Bruel & Kjaer 4507 B 005 in a chosen net of points on the upper face of the slab (27 cross-sections and 8 points in each cross-section) (Fig. 3). Later the measurement system was completed to eight transducers and so the whole cross-section can be measured at a time. The point of excitation was designed to be able to excite basic bending modes of natural vibration of the slab. Values of the Frequency Response Function were obtained as an average from ten measurements**.** The window length of the time signal processing was 32 s, the frequency range of the window was set to 400 Hz.

5 Modal characteristics evaluation and their mutual comparison

5.1 Reinforced concrete beams

The evaluation of natural frequencies and mode shapes of the reinforced concrete beams and slabs was done off line using program STAR (Spectral Dynamics). With regard to a frequency range of the dynamic analysis 0-200 Hz, four natural frequencies and mode shapes were evaluated after each load step for the reinforced concrete beams.

Modal characteristics, which were measured after each load step, were mutually compared using the same methods for all concrete elements. The change of modal characteristics was compared with the damage state of the elements (Fig. 4). For the comparison of natural modes, changes of a mode surface curvature $CAMOSUC_{(j),x}$ were used (Fig. 5 - 7)

$$CAMOSUC_{(j),x} = \left| \frac{r_{(j)X,x+1} - 2r_{(j)X,x} + r_{(j)X,x-1}}{h^2} - \frac{r_{(j)Y,x+1} - 2r_{(j)Y,x} + r_{(j)Y,x-1}}{h^2} \right|, \quad 2)$$

where $r_{(j),XX,x}$ is the value of the j-th natural mode shape in the x-th measured point in one damage (or virgin) state XX of the beam, $r_{(j),YY,x}$ is the value of the j-th natural mode shape in the x-th measured point in another damage state YY of the beam and h is the dimension of the net of measured points.

Then the changes of a modal flexibility matrix $[\delta]$ (Fig. 8) were used for comparison of natural modes

$$[\boldsymbol{\delta}] = [\mathbf{R}_{(j)}][\mathbf{1/\omega}^2_{(j)}][\mathbf{R}_{(j)}]^T, \quad (3)$$

where $[R_{(j)}]$ is the modal matrix composed of n measured natural modes and $[1/\omega^2_{(j)}]$ is the diagonal matrix composed of natural angular frequencies $\omega^2_{(j)}$.

The last method used for comparison of natural modes was the second derivative of changes of diagonal members of a modal flexibility matrix $\Delta[\delta]''$ (Fig. 9)

$$\Delta\delta''_r = \frac{\Delta\delta_{r,x+1} - 2\Delta\delta_{r,x} + \Delta\delta_{r,x-1}}{h^2}, \quad (4)$$

where $\Delta\delta_{r,x}$ is the change of the diagonal member r of the modal flexibility matrix and h is the distance of the net of measured points.

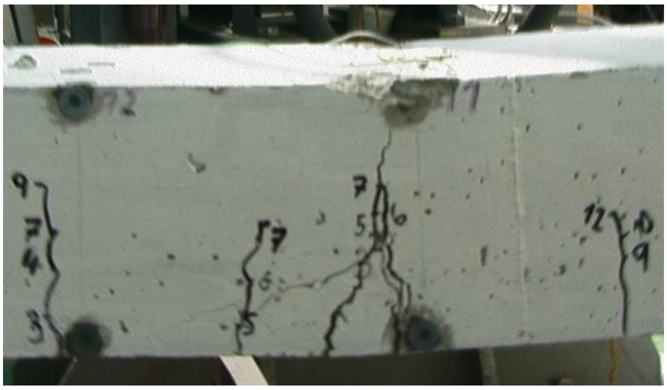

Fig. 4 Reinforced concrete beam No. 3. The marked cracks and the final crack in the cross-section No. 11

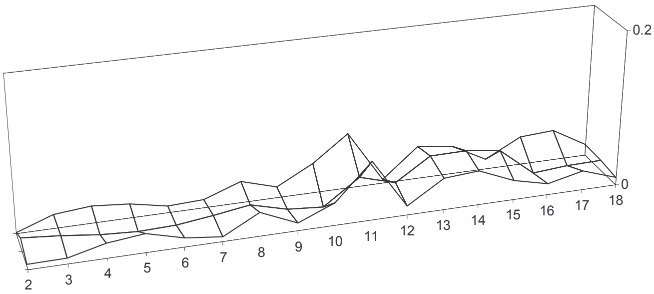

Fig. 5 The function CAMOSUC$_{(1),x}$, comparison between the virgin and the last states– the beam No. 3

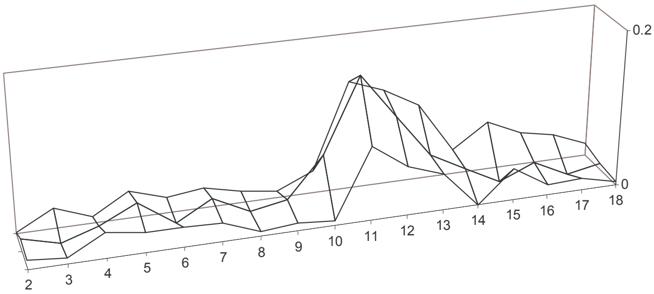

Fig. 6 The function CAMOSUC$_{(2),x}$, comparison between the virgin and the last states – the beam No. 3

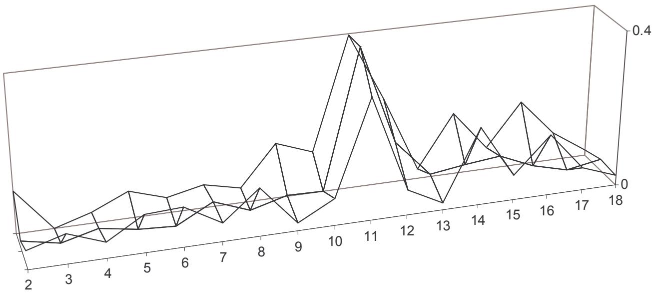

Fig. 7 The function CAMOSUC$_{(3),x}$, comparison between the virgin and the last states – the beam No. 3

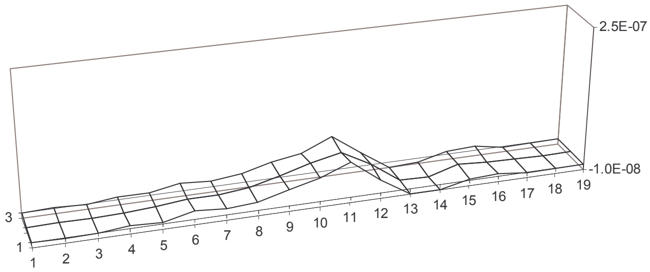

Fig. 8 The $\Delta[\delta]$, comparison between the virgin and the last state – the beam No. 3

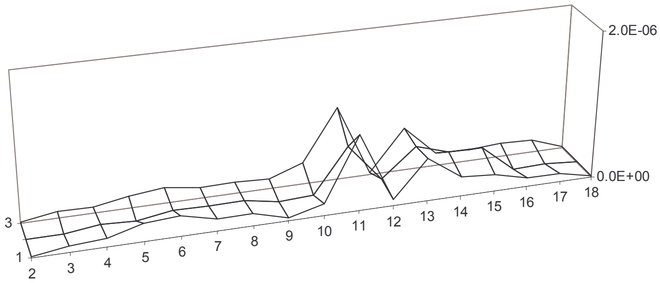

Fig. 9 The $\Delta[\delta]''$, comparison between the virgin and the last state – the beam No. 3

5.2 Reinforced concrete slabs

The evaluation of natural frequencies and mode shapes of the reinforced concrete slabs was done with the same equipment and the same frequency range as for the previous beams. Five natural frequencies and mode shapes were evaluated after each step of loading for the reinforced concrete slabs and they were mutually compared using the same functions as for the beams (Fig. 11 – 15). The position of the higher values of these functions were compared with marked position of cracks (Fig. 10) and after the final load step with the position of the final crack (Fig. 10).

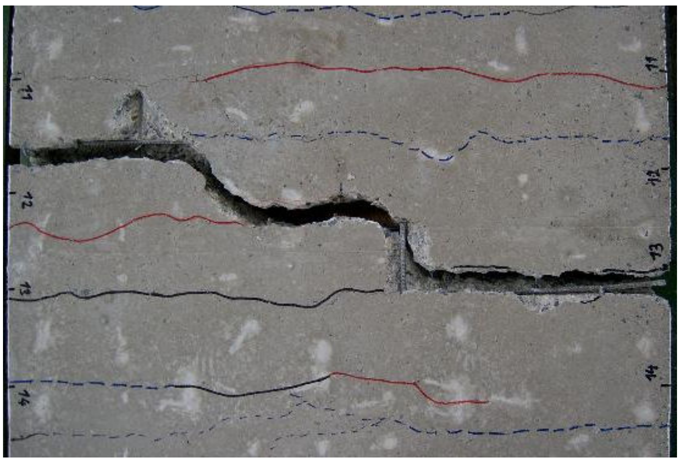

Fig. 10 Reinforced concrete slab No. 4. The marked cracks and the final crack between the cross-sections No.12 and 13.

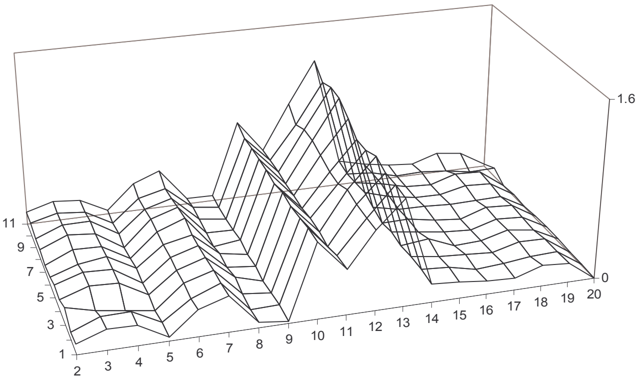

Fig. 11 The function $CAMOSUC_{(1),x}$, comparison between the virgin and the last states– the slab No. 4

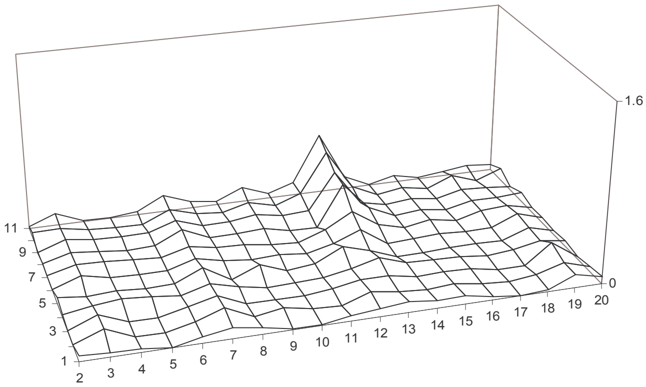

Fig. 12 The function $CAMOSUC_{(2),x}$, comparison between the virgin and the last states – the slab No. 4

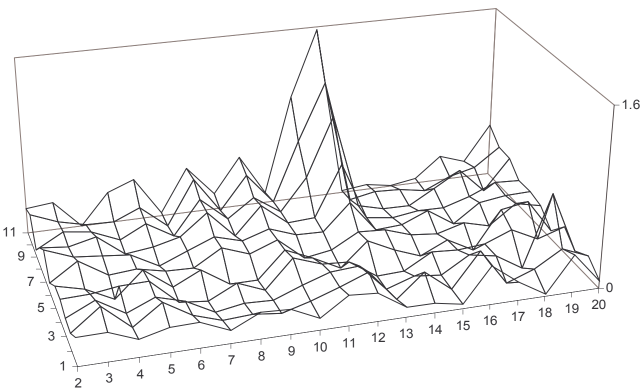

Fig. 13 The function $CAMOSUC_{(3),x}$, comparison between the virgin and the last states – the slab No. 4

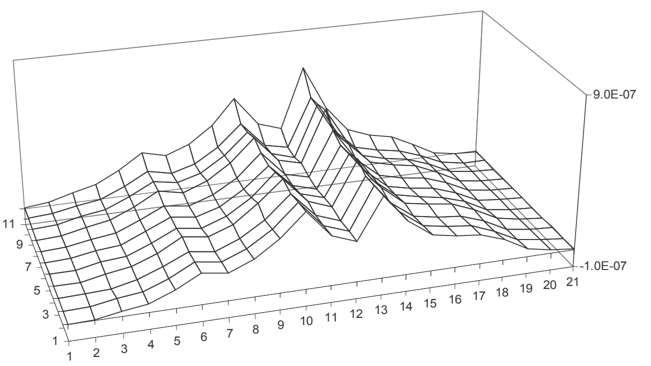

Fig. 14 The Δ[δ], comparison between the virgin and the last states – the slab No. 4

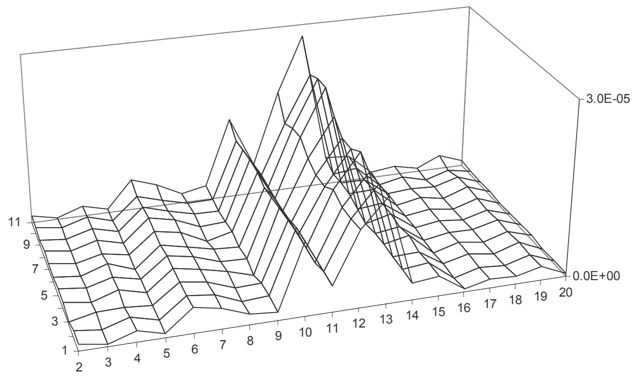

Fig. 15 The Δ[δ]″, comparison between the virgin and the last states – the slab No. 4

5.3 Prestressed concrete slabs

For modal characteristic evaluation of the prestressed concrete slabs the new equipment with program ME ScopeVES (Bruel & Kjaer) was used. With regard to a frequency range of the dynamic analysis 5-400 Hz, nine natural frequencies and mode shapes were evaluated after each step of loading for the prestressed concrete slabs and they were mutually compared using the same functions as for the reinforced concrete beams and slabs (Fig. 16 – 20).

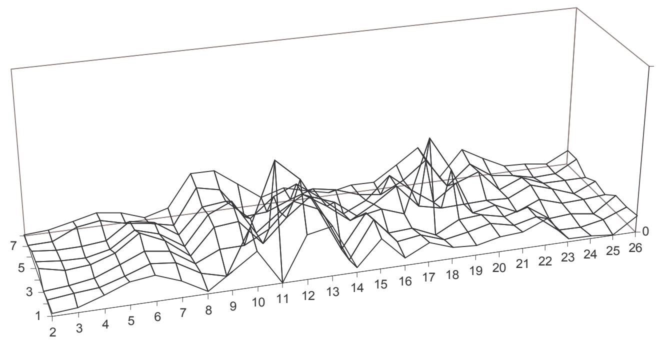

Fig. 16 The function $CAMOSUC_{(1),x}$, comparison between the virgin and the state after 3 500 000 loading cycles– the prestressed concrete slab No. 1

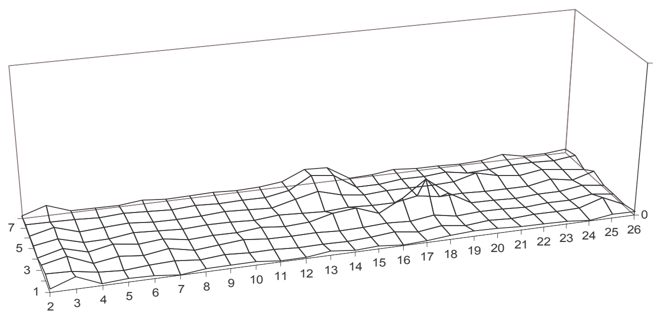

Fig. 17 The function $CAMOSUC_{(2),x}$, comparison between the virgin and the state after 3 500 000 loading cycles – the prestressed concrete slab No. 1

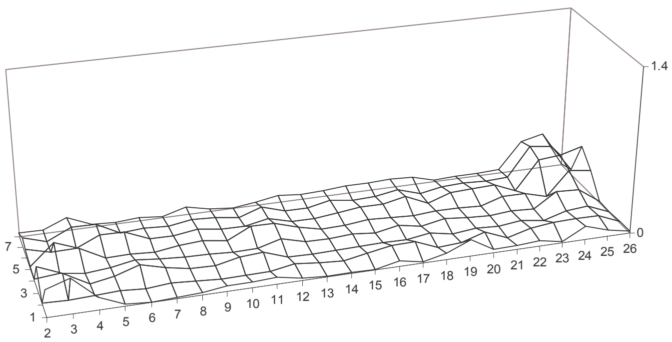

Fig. 18 The function $CAMOSUC_{(3),x}$, comparison between the virgin and the state after 3 500 000 loading cycles – the prestressed concrete slab No. 1

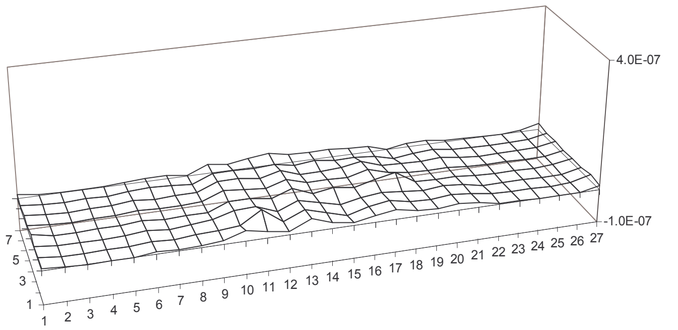

Fig. 19 The $\Delta[\delta]$ between the virgin state and the state after 3 500 000 loading cycles of the prestressed concrete slab No. 1

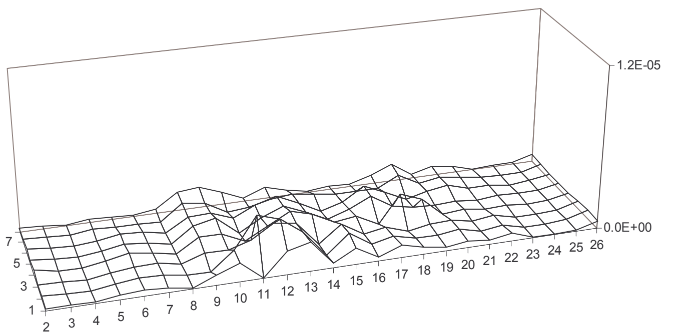

Fig. 20 The $\Delta[\delta]''$ between the virgin state and the state after 3 500 000 loading cycles of the prestressed concrete slab No. 1

6 Conclusion

The dynamic behavior changes of three types of concrete elements in dependence on their damages caused by static and dynamic loading were investigated. The position and the size of cracks were marked on the elements during each static load step (Fig.4, 10). After unloading, all cracks closed and were invisible. All measurements of modal characteristics were done before the cracks started to be visible by eye in unloaded state.

Three different methods were used for damage identification and localization: CAMOSUC, $\Delta[\delta]$ and $\Delta[\delta]''$. Based on the position and on the size of the evaluated values from each method, the identification of the damage of the elements was done. The results were compared with the marked positions of the damages or with the final crack after the end of the dynamic fatigue loading.

For the function CAMOSUC(j),x, the position of cracks, especially the final crack (Fig.4, 10), agrees with the higher values (Fig. 5-7 and Fig. 11-13) of this function. Nevertheless, for the lower damage as for the fatigue damage of the prestressed concrete slab this function gives worse results (Fig. 16 – 18). The $\Delta[\delta]$ describes well the increase of the flexibility of the damage domain of the elements (Fig. 8, Fig. 14, Fig. 19). The extreme values $\Delta[\delta]''$ (Fig. 9, Fig. 15, Fig. 20) prove good agreement with the position of the cracks.

For acquisition of reliable data for appreciation of monitored structure based on $\Delta[\delta]$ and $\Delta[\delta]''$ it is very important to consider carefully the character and number of natural modes, which are used in their computation. For reliable analysis, it is important to obtain reference data about dynamic properties of an investigated structure in the virgin state, optimally before starting its operation.

The investigation was supported by Czech Science Foundation as the project No. 103/05/P302 „Damage detection of a prestressed concrete element based on dynamic characteristics changes."

References:

[1] Brincker, R. - Andersen, P. - Cantieni, R.: Identification and Level I Damage Detection of the Z24 Highway Bridge, *Experimental Techniques*, Vol. 25. No. 6, 2001, pp. 51-57.

[2] Farrar, C.R. - Jauregui, D.A.: Comparative Study of Damage Identification Algorithms Applied to a Bridge: I Experiment, *Smart Materials and Structures*, Vol. 7, 1998, pp.704-719.

[3] Feltrin, G. - Motavalli, M.: Vibration-based Damage Detection on a Highway Bridge, *Proc. of the 1st Int. Conf. on Bridge Maintenance, Safety and Management*, Barcelona, Spain, 2002.

[4] Fryba,L. - Pirner,M. - Urushadze,S.:Localization of damages in concrete structures, *Proc. of the Int. Conf. Computational Methods and Experimental Measurements X*, 2001.

[5] Maia, N. – Silva, J.: Theoretical and Experimental Modal Analysis, *Textbook*, Research Studies Press Ltd. Taunton, England. 1997.

[6] Pandey, A. K.-Biswas, M: Damage detection in Structures Using Changes in Flexibility. Journal of Sound and Vibration, 169, pg. 3 – 17, 1994.

[7] Plachy, T.: Dynamic study of a reinforced concrete beam damaged by cracks, *PhD thesis*, CTU in Prague, 2003.

[8] Salawu, O. S.-Williams, C.: Damage Location Using Vibration Mode Shapes. *Proc. of the 12th Int. Modal Analysis Conference*, pp. 933-939, 1994.